AAC Accepted Manuscript Posted Online 25 July 2016
Antimicrob. Agents Chemother. doi:10.1128/AAC.00190-16

Antimicrobial Agents and Chemotherapy: Article

Exploiting interkingdom interactions for the development of small molecule inhibitors of *Candida albicans* biofilm formation

F. Jerry Reen[1], John P. Phelan[1], Lorna Gallagher[1], David F. Woods[1], Rachel M. Shanahan[2], Rafael Cano[2], Eoin Ó Muimhneacháin[2], Gerard P. McGlacken[2] and Fergal O'Gara[1,3#].

[1] BIOMERIT Research Centre, School of Microbiology, University College Cork - National University of Ireland, Cork, Ireland.

[2] School of Chemistry and Analytical and Biological Chemistry Research Facility (ABCRF), University College Cork - National University of Ireland, Cork, Ireland.

[3] School of Biomedical Sciences, Curtin Health Innovation Research Institute, Curtin University, Perth, WA 6102, Australia.

Running Head: Hydroxy Alkylquinolone signals target *Candida* biofilm.

FJR and JPP contributed equally to this work.

To whom correspondence should be addressed. Mailing address: Prof. Fergal O'Gara, BIOMERIT Research Centre, School of Microbiology, University College Cork, Ireland. Phone number: + 353-21-4901315; Fax number: + 353-21-4275934; E. mail: f.ogara@ucc.ie.

Abstract

A rapid decline in the development of new antimicrobial therapeutics has coincided with the emergence of new and more aggressive multidrug resistant pathogens. Pathogens are protected from antibiotic activity by their ability to enter an aggregative biofilm state. Therefore, disrupting this process in pathogens is a key strategy for the development of next generation antimicrobials. Here we present a suite of compounds, based on the *Pseudomonas aeruginosa* 2-heptyl-4(1H)-quinolone (HHQ) core quinolone interkingdom signal structure, that exhibit non-cytotoxic anti-biofilm activity towards the fungal pathogen *Candida albicans*. In addition to providing new insights into what is a clinically important bacterial-fungal interaction, the capacity to modularize the functionality of the quinolone signals is an important advance in harnessing the therapeutic potential of signaling molecules in general. This provides a platform for the development of potent next generation small molecular therapeutics targeting clinically relevant fungal pathogens.

41 **Introduction**

42 With the ever increasing emergence of antibiotic resistant pathogens and the lack of new
43 antibiotics coming to market, we are entering a 'post-antibiotic era' (1-3). This realization has
44 underpinned a global initiative to identify new and innovative approaches to infection
45 management. As such, targeting virulence as a potential strategy for developing new anti-
46 microbial drugs has been the focus of several research initiatives (4-11). In principle, suppressing
47 virulence behavior and locking pathogens in a vegetative non-biofilm forming lifestyle renders
48 them less infective and more susceptible to conventional antibiotics (4, 12). While some success
49 has been achieved against bacterial pathogens (6, 10, 13-19), less focus has been placed on
50 fungal infections which nevertheless continue to cause serious complications and mortality in
51 patients (8, 20-22). Indeed, despite the medical and economic damage caused by fungal biofilms,
52 there remains an urgent and largely unmet need for the identification of compounds able to
53 specifically and selectively target and inhibit this mode of growth in clinically relevant fungal
54 pathogens (23).

55 The predominant nosocomial fungal pathogens, which include *Candida* spp., *Aspergillus* spp.,
56 and *Fusarium* spp., are difficult to diagnose and cause high morbidity and mortality, even
57 following antifungal therapy (21). *Candida albicans* causes a variety of complications ranging
58 from mucosal disease to deep seated mycoses, particularly in immunocompromised individuals
59 (21, 24). Along with other fungal and yeast pathogens, *C. albicans* are known to form structured
60 communities known as biofilms on medical devices either pre- or post-implantation leading to
61 recurring infections and in some cases death (25, 26). Once established in the biofilm phase, *C.*
62 *albicans* presents a significant clinical problem with current treatment options severely limited

63 by the intrinsic tolerance of fungal biofilms to antimycotics (20, 27, 28). Recent combination
64 therapies incorporating antibacterial and antifungal agents have provided some success (29).
65 However, as with all antibiotic based strategies, reports of resistance continue to emerge (27),
66 and biofilms themselves are considered a breeding ground for the emergence of antibiotic
67 resistant strains, effectively hastening the onset of the perfect storm whereby the rapid decline in
68 new antibiotic production has been met by an equally rapid increase in multidrug resistant
69 organisms (1). Thus the need to consider new anti-infective strategies that do not target essential
70 processes in the target organism. While blocking biofilms in these organisms' remains a major
71 clinical challenge (26, 30), exploiting our increased understanding of microbial signaling
72 networks to control virulence and biofilm behavior is one innovative approach with significant
73 potential.
74 Many sites of infection are colonized by communities of mixed fungal and bacterial organisms,
75 and several layers of communication impact significantly on the dynamics and flux of these
76 populations (31, 32). For example, *C. albicans* is known to co-exist with *Pseudomonas*
77 *aeruginosa* in the cystic fibrosis (CF) lung, and interkingdom communication between the two
78 organisms has previously been reported (16, 33). The Pseudomonas Quinolone Signal (PQS), 2-
79 heptyl-3-hydroxy-4-quinolone, and its biological precursor 2-heptyl-4-quinolone (HHQ) are
80 important virulence factors produced by *P. aeruginosa*. Structurally, PQS and HHQ differ by the
81 presence of a hydrogen at C3 in HHQ and a hydroxyl group in PQS, giving rise to the increased
82 interest in modulating this position to assign biological function to the structure of these
83 molecules (34-37). Previously, we have shown that HHQ, but not PQS, suppresses biofilm
84 formation of *C. albicans* (10). In response, *C. albicans* produces farnesol which has been shown

to modulate PQS production in *P. aeruginosa* (33). As both PQS and HHQ promote virulence and pathogenicity of *P. aeruginosa* (38, 39), their utility as an anti-*Candida* treatment falls short of being a viable anti-fungal treatment. However, the amenability of these small molecules to chemical modification provides an opportunity to develop compounds with specificity of function.

The transcriptional data and microscopic imaging described in this study have implicated components of the cell wall as key factors in the response of *C. albicans* to *P. aeruginosa* alkylhydroxyquinolone (AHQ) signaling. Furthermore, the biological activity of each class of analogue in bacterial, fungal and host systems provides a new insight into the possible interkingdom role of AHQs, particularly in a clinical setting such as the CF lung where all three systems co-exist. From a translational perspective, lead HHQ analogues were identified with four key features: (1) potent anti-biofilm activity towards *C. albicans*, (2) selective non-cytotoxicity towards mammalian cell lines, (3) non-agonistic and (4) potentially antagonistic to the virulent pathogen *P. aeruginosa*. Several analogues retained the significant potency of the parent HHQ molecule against *C. albicans* biofilm formation, whilst simultaneously becoming inactive in *P. aeruginosa* quorum sensing. This suggests that these molecules have the potential to be further optimized for use as anti-*Candida* infectives without the concomitant limitation of *P. aeruginosa* virulence augmentation.

Materials and Methods

***C. albicans* stock maintenance and culturing conditions**.

106 *C. albicans* strain SC5314 was sub-cultured from 15% (v/v) glycerol stocks at -80°C onto Yeast
107 Peptone Dextrose (YPD) medium [1% (w/v) yeast extract, 2% (w/v) peptone and 2% (w/v)
108 dextrose] and incubated at 30°C overnight.

109 ***P. aeruginosa* stock maintenance and culturing conditions.**

110 *P. aeruginosa* strains, PAO1 and *pqsA*$^-$ mutant, containing the chromosomally inserted *pqsA-*
111 *lacZ* promoter fusion on plasmid pUC18-mini-Tn7, were maintained on Luria Bertani (LB) agar
112 plates, supplemented with carbenicillin (200 µg/ml) and X-gal (40 µg/ml), and incubated at 37°C
113 overnight. Single colonies were inoculated into LB broth (20 ml), supplemented with
114 carbenicillin (200 µg/ml), and incubated at 37°C, shaking at 180 rpm overnight. For subsequent
115 experiments, the OD_{600nm} was recorded and a starting OD_{600nm} of 0.02 was inoculated into fresh
116 LB broth, supplemented with carbenicillin (200 µg/ml) and incubated at 37°C, shaking at 180
117 rpm.

118 **Structural modification of HHQ**

119 The synthesis of HHQ, PQS (40, 41) and other HHQ-based analogues (36, 37) was carried out
120 via previously described methods. Novel compounds and compounds which required modified
121 syntheses are described *vide infra* and in the supporting information (**Supplemental Data**).

122 **Thin Layer Chromatographic (TLC) analysis**.

123 Silica TLC plates, activated by soaking in 5% (w/v) K_2HPO_4 for 30 min were placed in an oven
124 at 100°C for 1 hr (42). Analogues (5 µl, 10 mM) were spotted approximately 1 cm from the
125 bottom. The spots were dried and the plate placed in a mobile phase comprising 95:5

126 dichloromethane:methanol. The plate was viewed under UV light when the mobile phase had run
127 5 cm below the top of the plate.

128 **Biofilm formation, quantification, and visualization**.

129 *C. albicans* biofilm formation was carried out in 96 well plates, as previously described (43).
130 Seeding densities for all subsequent experiments (n=3) were OD_{600nm} 0.05. Biofilm formation
131 was measured as previously described using a semi-quantitative tetrazolium salt, 2,3-bis-(2-
132 methoxy-4-nitro-5-sulfophenyl)-2H tetrazolium-5-carboxanilide inner salt (XTT) reduction assay
133 (44). Experiments were repeated at least three times, with at least eight technical replicates.
134 Visualization of biofilm formation was performed on glass coverslips in 6-well plates using
135 Confocal Scanning Laser Microscopy (CSLM). All images were captured using the Zeiss HBO-
136 100 microscope illuminating system, processed using the Zen AIM application imaging program
137 and converted to JPGs using Axiovision 40 Ver. 4.6.3.0. A minimum of three independent
138 biological repetitions were carried out.

139 **Viable colony biofilm assay**

140 *C. albicans* biofilms, supplemented with analogues and parent compounds, were grown in 6-well
141 plates and incubated overnight at 37°C. Briefly, *C. albicans* Yeast Nitrogen Base (YNB) cultures
142 were measured at OD_{600nm}, diluted to 0.05 in YNB-NP supplemented with analogues, plated onto
143 6-well plates and incubated for 1 hr at 37°C. Media was removed, wells were washed twice with
144 sterile PBS and supplemented with fresh YNB-NP with analogues. Plates were incubated
145 overnight at 37°C after which media was removed and wells washed with sterile PBS. For serial
146 dilutions, biofilms were cell-scraped into 1 ml PBS, vortexed, and serially diluted into sterile

147 PBS. Serial dilutions were plated (100 µl) onto YPD agar and incubating overnight at 37°C.
148 Colonies were counted and recorded the next day.

149 ***C. albicans* growth curves**

150 Overnight *C. albicans* cultures grown in YNB were diluted to 0.05 in YNB supplemented with
151 analogues. Cultures (200 µl) were added to each well of a 100 well plate and grown for a 24 hr
152 period on a Bioscreen C spectrophotometer (Growth Curves USA).

153 **RNA isolation and qRT-PCR transcriptional analysis**.

154 Overnight *C. albicans* cultures were diluted to 0.05 at OD_{600nm} in either YNB or YNB-NP
155 (Difco). YNB cultures were supplemented with methanol whereas YNB-NP cultures were
156 supplemented with either 100 µM HHQ or the methanol volume equivalent. Cultures were
157 grown at 37ºC with agitation (180 rpm) for 6 hr after which they were centrifuged at 4000 rpm,
158 supernatants discarded and pellets frozen at -20ºC until processing. RNA was isolated using the
159 MasterPure Yeast RNA purification kit (Cambio Ltd, Cambridge UK) according to
160 manufacturer's specifications, and was quantified using a ND-1000 Spectrophotometer
161 (NanoDrop Technologies, USA). Genomic DNA was enzymatically removed using Turbo DNA-
162 free DNase (Ambion), and samples were confirmed DNA free by PCR. RNA was converted to
163 cDNA using random primers and AMV reverse transcriptase (Promega) according to
164 manufacturer's instructions. qRT-PCR was carried out using the Universal ProbeLibrary (UPL)
165 system (Roche) according to manufacturer's specifications, and samples were normalized to *C.*
166 *albicans* actin transcript expression (*ACT1*). A full list of primers and UPL probes used in this
167 study is detailed in Supplemental Table 1.

168 **Phenazine extraction**.

169 *P. aeruginosa* strains were cultured as described above for 24 hr, with the addition of analogues
170 (100 µM), and pyocyanin was extracted as described previously (45). Cultures were centrifuged
171 at 4000 rpm for 10 minutes and the cell free supernatant (5 ml) removed. Chloroform (3 ml) was
172 added, and mixed by vortex. After centrifugation at 4000 rpm for 5 min, the lower aqueous phase
173 was transferred to 0.2 M HCl (2 ml). Samples were mixed by vortex and centrifuged at 4000 rpm
174 for 5 min to separate the phases. An aliquot of the top phase (1 ml) was removed and
175 spectrophotometrically analyzed at OD_{570nm}. Phenazine production was calculated using the
176 following formula: OD_{570nm} x 2 x 17.072 and the units expressed in µg/ml.

177 **Promoter fusion based expression analysis**.

178 Promoter fusion analyses were performed in a 96-well format, with β-galactosidase activity
179 measured as described previously (46). Briefly, overnight cultures of wild-type *PAO1 pqsA-lacZ*
180 (pLP0996) and mutant strain PAO1 *pqsA*$^-$ *pqsA-LacZ* were diluted to OD_{600nm}=0.02 in LB.
181 Analogues at 100 µM final concentration were added, mixed, aliquoted into 96 well plates and
182 incubated overnight at 37ºC with shaking. The next day, OD_{600nm} values were recorded in a plate
183 reader. Aliquots of cells (0.02 ml) were permeabilized [100 mM dibasic sodium phosphate
184 (Na_2HPO_4), 20 mM KCl, 2 mM $MgSO_4$, 0.8 mg/mL CTAB (hexadecyltrimethylammonium
185 bromide), 0.4 mg/mL sodium deoxycholate, 5.4 µL/mL beta-mercaptoethanol] and added to
186 substrate solution [60 mM Na_2HPO_4, 40 mM NaH_2PO_4, 1 mg/mL o-nitrophenyl-β-D-Galactoside
187 (ONPG), 2.7 µL/mL β-mercaptoethanol]. The kinetics of color development was monitored and
188 the reactions were stopped using 1M $NaCO_3$. OD_{420nm} were recorded as above. Miller units were

189 calculated using the following equation; 1000 x [OD_{420nm}/(OD_{600nm}) x 0.02 ml x reaction time
190 (min)].

191 **Cytotoxicity Assay.**

192 Lactate dehydrogenase (LDH) release from a panel of mammalian cells was assayed as a
193 measure of cytotoxicity using an LDH colorimetric kit (Roche) according to manufacturers'
194 instructions (36). Briefly, IB3-1 lung epithelial cells, A549 human lung adenocarcinoma
195 epithelial cells, DU-145 human prostate cancer cells and HeLa cervical cancer cells were seeded
196 onto 96 well plates and treated with methanol (control) and analogues. Following 16 hr
197 incubation at 37°C and 5% CO_2, supernatants were removed and added to catalyst reaction
198 mixture in a fresh plate and further incubated at 37°C and 5% CO_2 for 30 min to allow for color
199 development. After this period, the plate was analyzed on an ELISA plate reader at OD_{490nm}.
200 Cytotoxicity was expressed as a percentage of cells treated with 0.1% (v/v) Triton (100%
201 cytotoxicity).

202 **Statistical analysis**.

203 All graphs were compiled using GraphPad Prism (version 5.01) unless otherwise stated. All data
204 were analyzed using built-in GraphPad Prism (version 5.01) functions as specified. The level of
205 significance was set at $p = 0.05$ (*) and post-hoc comparisons between groups were performed
206 using the Bonferroni multiple-comparison test.

207

208

209

210

Results

Key modifications of the quinolone framework retain anti-biofilm activity towards *C. albicans*

The HHQ molecule has previously been shown to suppress biofilm formation in *C. albicans* at concentrations from 10 – 100 µM (2.47 – 24.7 µg/ml) independent of any effects on the growth of planktonic cells (10). Previous structure function analysis of the activity of the quinolone framework had implicated the C-3 position as a key component of interspecies anti-biofilm activity (36). We undertook further modification of the HHQ parent molecule with the aim of developing viable anti-biofilm compounds to target *C. albicans*. These compounds were incorporated into a larger collection of alkylquinolone analogues, systematically modified at different positions on the molecule and classified on the basis of their substitutions relative to the parent framework HHQ (**Table 1**).

The suite of analogues was first tested to establish their potency as anti-biofilm compounds against *C. albicans* using an optimized XTT assay, a commonly used quantitative method to assess *Candida* biofilm mass and growth (47). As previously described (10), HHQ significantly suppressed biofilm formation when compared to untreated and methanol treated cells, whereas PQS appeared to induce biofilm formation (**Figure 1**). When all analogues were similarly screened by XTT assay, several had similar anti-biofilm activity to HHQ [**1** and **2** (class I; modified at C-3)], **3, 4**, **6**, **7**, **9** (class II; modified anthranilate ring), and **12** (class III; modified alkyl chain) (**Figure 2a**). These analogues were diverse members of classes I, II, and III

233 suggesting that several components of the HHQ framework contribute to anti-biofilm activity of
234 the parent compound. A number of substitutions led to intermediate anti-biofilm activity,
235 including **5**, **8**, **10**, **11**, (class II; modified anthranilate ring) and **15** (class V; modified
236 anthranilate ring and alkyl chain length), while some analogues had completely lost the ability to
237 suppress *C. albicans* biofilm formation e.g. **13** (class IV; modified C-4), and the class V
238 compounds **14**, **16**, and **17** (**Figure 2a**). While modification of the C-3 position to produce PQS
239 led to loss of anti-biofilm activity (**Figure 1**), incorporation of an –N-NH_2 moiety (**2**) at the 3-
240 position or substitution of C-3 with NH (**1**), did not affect the ability to suppress *C. albicans*
241 biofilm formation (**Figure 2a**). Addition of Cl at the C6 and C8 positions of the anthranilate ring
242 (**6** and **7**) also did not lead to loss of anti-biofilm activity. In contrast, the introduction of
243 considerable steric bulk with the addition of an *n*-hexyl alkyl chain at C6 of the anthranilate ring
244 (**5**), or elaboration of the aromatic group as with the naphthyl compound (**8**), resulted in
245 compounds with significantly less potent anti-biofilm activity relative to HHQ. These data
246 suggest an exquisite level of specificity for the interaction between HHQ and the *C. albicans*
247 biofilm intracellular machinery. Modification of the C2 alkyl chain from *n*-heptyl (HHQ) to *n*-
248 nonyl C9 (**12**) did not affect anti-biofilm activity, while parallel modification of the anthranilate
249 ring resulted in a complete loss, as with the Class V compounds **16** or **17**. Modifying the C-4
250 position (C=O to C=S) (**13**), the quinolone thiol exhibited an increase in XTT activity ($P<0.05$)
251 relative to controls (**Figure 2a**), comparable to the increase observed in the presence of PQS
252 (**Figure 1**). Previously, we have shown that HHQ elicits a dose-dependent reduction in *C.*
253 *albicans* biofilm formation (10). In order to determine if this also applied to the analogues that
254 retain anti-biofilm activity, dose response analysis of selected compounds **1**, **2**, **4**, **6**, and **12**

255 representing classes I, II, and IV, was undertaken. This revealed compound specific responses,
256 with 10 μM of compounds **2**, **4**, and **12** being sufficient to elicit a statistically significant
257 reduction in biofilm formation (**Figure 2b**). All five compounds reduced biofilm formation when
258 applied at 50 μM and 100 μM. To further confirm the anti-biofilm activity of the lead
259 compounds, viable colony counts were performed on selected analogues using the maximum 100
260 μM compound dose. This confirmed the outputs from the XTT assays; all analogues, along with
261 HHQ, significantly reduced viable biofilm cells in comparison to the control (**Figure S1a**).
262 Importantly, the anti-biofilm activity was found to be independent of planktonic growth, which
263 was unaffected in the presence of selected compounds (**Figure S1b**).

264

265 **Microscopic staining reveals structural changes in *C. albicans* biofilms**

266 The formation of biofilms in bacteria, yeast and fungi is a highly ordered process involving
267 multicellular behavior and has been defined in several stages (22). Confocal microscopy
268 combined with intracellular staining was used to assess structural integrity and cellular
269 morphology of *C. albicans* incubated on coverslips. Biofilms were individually stained with each
270 of the dyes and multiple fields of view were visualized to accurately represent the effect of the
271 analogues. The biofilm observed for methanol and untreated controls displayed all the
272 characteristics of a typical *C. albicans* biofilm and were classified as wild-type (**Figure 1**).
273 Calcofluor, Concanavalin A and FUN-1 staining revealed a uniform distribution of
274 chitin/cellulose and cell wall mannosyl/glucosyl residues indicative of viable wild-type
275 morphology (**Figure 1**). Those analogues identified by XTT assay as causing impaired biofilm

formation (**1, 2**, **3**, **4**, **6**, **7**, **9**, **12**, and **15)** exhibited markedly disrupted structures when grown on coverslips and were classified as atypical morphologies (**Figure 3**). Cells treated with class I analogues were found to be largely compromised in their biofilm forming capabilities and were classified as morphologically atypical. Biofilms produced with both **1** and **2** were significantly distorted, displaying a spindle-like phenotype. Hyphae were short in length, and predominantly displayed yeast cell types rather than hyphal structures. Other structure disrupting analogues were from Class II, III and V, suggesting that specific modifications on the anthranilate ring and alkyl chain variation do not significantly affect the anti-biofilm activity compared to the parent compound (**Figure 3**).

Some analogues, including those that exhibited intermediate activity in the XTT assay, did not alter the biofilm structure, with **5**, **11**, **13**, **14** and **16** all placed into the wild-type morphology group. Biofilms formed in the presence of **13** showed hyper-production of short hyphae, creating a dense mycelial network (**Figure S2**). The remaining analogues from Class II; **8** and **10** (**Figure S1**) caused significant biofilm disruption with fragmented hyphae, stunted vegetative growth and considerably large cell debris fields. Cells incubated with the Class V molecule **17** induced a severely compromised phenotype (**Figure S2**) where debris fields comprising yeast cells and blastospores characterized the structural phenotype.

Enhanced gene transcript expression of *HWP1*, *ECE1*, *ALS3*, *IHD1* and the uncharacterized open reading frame *ORF 19.2457* provides a molecular mechanism for alkyl quinolone activity towards *C. albicans*

297 In addition to providing new insights into the interkingdom relationship between these important
298 pathogens, there has recently been a strong emphasis placed on ligand receptor interactions and
299 the need to provide molecular mechanisms for the action of any potential therapeutic compound
300 (48). We previously implicated *TUP1* in the HHQ-mediated suppression of biofilm formation in
301 *C. albicans* suggesting a role for the cell-wall in this interaction (10, 16). More recently, several
302 reports have shown changes in expression of cell-wall associated genes linked to biofilm
303 formation in this organism (16, 20, 28, 49-51). These included a cohort of eight genes that are
304 proposed to constitute the core filamentous response network; namely *ALS3*, *ECE1*, *HGT2*,
305 *HWP1*, *IHD1*, *RBT1*, *DCK1*, and the gene of unknown function open reading frame *orf19.2457*
306 (51). Therefore, transcript expression of a cohort of genes implicated in cell wall biogenesis,
307 hyphal development, biofilm formation and other related functions that were previously shown to
308 be upregulated during the morphological transition from yeast to filamentous growth was
309 investigated (**Table S1**) (16, 51). The housekeeping gene *ACT1* was chosen for normalization
310 based on previous biofilm studies (52). We observed that several transcripts were hyper-
311 expressed in a HHQ dependent manner; specifically, *HWP1*, *ECE1, ALS3, IDH*1 and the as yet
312 uncharacterized open reading frame *(ORF) 19.2457* (**Figure 4**). The remaining transcripts
313 (*CPH1*, *EFB1*, *ESS1*, *RBT1*, *TUP1*, *BCR1*, *DCK1*, and *HGT2*) yielded expression patterns
314 similar to control cells (**Figure S3**). It was perhaps somewhat surprising that, while treatment of
315 *C. albicans* with *P. aeruginosa* supernatants has previously been shown to downregulate
316 expression of the *RBT1, RBT5* and *RBT8* genes (16), expression of *RBT1* was unaltered in the
317 presence of HHQ (**Figure S3**). Taken together, these data suggest that HHQ induces a specific
318 subset of cell wall proteins in *C. albicans*. Further work is needed to identify the upstream

319 components of this response, although *in silico* screening of *C. albicans* genome sequences has
320 ruled out the presence of an obvious PQS receptor (unpublished data).
321

322 **Lead compounds display reduced cytotoxic activity towards specific mammalian cell lines**

323 Evaluating the cytotoxicity of synthetic compounds is crucial in the context of developing
324 targeted and highly optimized molecular therapeutics that are benign to human cellular
325 physiology and ideal for use in a clinical environment. In previous work, we showed that
326 analogue **1** was significantly less cytotoxic than HHQ, with an 80% reduction in LDH release
327 relative to the parent compound (36). Therefore, the suite of analogues was tested for *in vitro*
328 cytotoxicity towards IB3-1 airway epithelial cells. Class I analogues exhibited reduced
329 cytotoxicity to IB3-1 cells with **2** displaying approximately 34% toxicity (**Figure 5a**). Several
330 class II analogues (**4**, **6**, and **9**) exhibited reduced cytotoxicity relative to IB3-1 cells treated with
331 HHQ, with **7** not reaching statistical significance. The class III analogue **12** was comparable to
332 HHQ. Of the analogues that did not retain anti-biofilm activity, **5, 8, 10** and **11** exhibited variable
333 cytotoxicity to IB3-1 cells whereas **13** exhibited considerably reduced cytotoxicity to IB3-1 cells
334 (**Figure S4**). Finally, **16** exhibited very low levels of cytotoxicity, while **17** was reduced relative
335 to HHQ treated cells. Compound **15** was the most toxic killing approximately 91% of all cells
336 (**Figure 5a**).

337 In order to achieve a more comprehensive understanding of the selective toxicity of the lead
338 compounds, several additional cell lines were tested (**Figure 5b**). LDH release assays were
339 performed in A549, DU145, and HeLa cell lines in the presence of 100 μM of the lead

compounds revealed distinct cytotoxicity profiles, with **1** and **9** consistently proving the least cytotoxic of the compounds tested. Compounds **4** and **6** exhibited reduced cytotoxicity in DU145 cells (although not statistically significant) but were comparable to HHQ in both the A549 and HeLa cell lines, while compound **2** exhibited increased cytotoxicity relative to HHQ in DU145 cells (**Table 2**). These data suggest that cell-specific cytotoxicity analysis will need to be performed prior to the introduction of these compounds in an applied setting.

HHQ analogues display a spectrum of agonist activity towards *P. aeruginosa* virulence.

Taken together, compounds **1**, **4**, **6**, and **9** pass both the first and second criteria described above, i.e. they retain anti-biofilm activity towards *C. albicans* while exhibiting reduced selective cytotoxicity towards specific host cell lines. However, both HHQ and PQS are co-inducers of the virulence associated LysR-Type Transcriptional Regulator; PqsR (41). The structural moieties that underpin the interaction between HHQ/PQS and PqsR remain to be fully characterized, although recent studies have reported diverse classes of PqsR antagonist (53-55), and implicated the hydrophobic pocket situated within the PqsR protein (56). Therefore, in order to assess whether the lead compounds could elicit a virulence response from *P. aeruginosa*, phenazine production and *pqsA* promoter activity (57) were monitored in a *pqsA* mutant where the capacity to produce native HHQ and PQS had been lost.

Both HHQ and PQS restored phenazine production in the *pqsA*- strain (**Figure 6A**). In contrast, the majority of analogues did not restore phenazine production in this strain, with the notable exception of compound **9**. Several analogues from different classes did partially restore

361 phenazine production in the mutant background, including **10**, **12**, and **17** (**Figure 6** and **Figure**
362 **S5**). None of the analogues interfered with phenazine production in the wild-type PAO1 strain,
363 suggesting that they are ineffective as PQS antagonists (**Figure S5**).

364 Similarly, while some degree of PqsR agonist activity was observed in the presence of
365 compounds **6**, **9**, **10**, **12**, **13**, and **17**, only HHQ and PQS significantly induced promoter activity.
366 All other analogues did not influence promoter activity in this system (**Figure 6B** and **Figure**
367 **S5**). Somewhat surprisingly, antagonistic activity towards *pqsA* promoter activity was not
368 observed, with almost all analogues failing to significantly suppress *pqsA* promoter activity in
369 the wild-type strain (**Figure S5**). The relative ineffectiveness of these analogues as PQS
370 antagonists may in part be due to hydroxylation of HHQ analogues (H at C3) to PQS analogues
371 (OH at C3), thus establishing the non-antagonistic behavior explained by a recent report by Lu
372 and colleagues, where the action of PqsH rendered anti-PQS compounds ineffective through
373 bioconversion (55).

374

375 **Discussion**

376 Current antimicrobial therapies tend to be non-pathogen-specific and there is evidence to suggest
377 that the availability of relatively non-toxic broad-spectrum therapies has contributed to the
378 emergence of resistance among both targeted and non-targeted microbes (58, 59). Consequently,
379 there is an urgent need to innovate new options for the targeted prevention of microbial infection
380 while avoiding the inevitable emergence of resistance that is the hallmark of broad spectrum
381 antibiotic therapies (59, 60). Increasingly, industry, academia and regulatory bodies have become
382 interested in single-pathogen therapies to treat highly resistant or totally resistant bacterial

383 pathogens, rightly viewed as an area of high unmet need (61-63). Exploiting interkingdom
384 communication networks, and the mode of action of the chemical messages or signals employed
385 therein, offers us a powerful platform from which to deliver on this.
386 Previously we had shown that the HHQ interkingdom signal molecule from *P. aeruginosa* could
387 suppress biofilm formation in *C. albicans* at concentrations ranging from 10 - 100 µM (2.47 –
388 24.7 µg/ml) (10). This suppression occurred independent of any growth limitation in planktonic
389 cells, and morphogenesis on spider media was also found to be unaffected (10). The design and
390 subsequent analysis of a suite of analogues based on the core HHQ quinolone framework has led
391 to the identification of several lead compounds that retain anti-biofilm activity towards *C.*
392 *albicans* but exhibit significantly reduced cytotoxicity towards IB3-1 epithelial cells when
393 compared with the parent HHQ molecule (data not shown). The selective cytotoxicity of the lead
394 compounds together with the dose dependent anti-biofilm effects will be key considerations in
395 determining the cell line specific therapeutic index of lead analogues as part of the ongoing
396 development of these compounds. Furthermore, unlike HHQ, these lead compounds are now
397 inactive towards the *P. aeruginosa* PqsR quorum sensing system, a critical requirement for their
398 potential future development as anti-biofilm therapeutics. In addition, the ability to generate
399 hydrochloride salts of the compounds ((36) and data not shown) suggests that solubility of future
400 therapeutics based on these scaffolds will not be a bottleneck. Several strategies have been
401 proposed for the implementation of anti-biofilm compounds as clinical therapeutics to target *C.*
402 *albicans* biofilm infections (64). As the HHQ analogues possess anti-biofilm, but not anti-
403 *Candida* activity, they would disrupt the formation of biofilms but not likely remove the
404 planktonic cells that remain at the site of infection. Therefore, combination with conventional

anti-fungal compounds would be required for effective clearance. Alternatively, where the potency of the anti-biofilm activity can be synthetically enhanced through further derivatization, clearance by the immune system might also be realistic.

The molecular mechanisms through which AHQs and the lead compounds identified in this study disrupt the formation of biofilms by *C. albicans* remains to be fully elucidated. Previously we have shown that HHQ does not affect adhesion, but rather impacts directly on the subsequent developmental stages in a TUP1-dependent manner (10). In this study we have shown that the expression of several cell-wall associated genes is increased in response to HHQ during the switch to hyphal growth. These genes have previously been implicated in the formation of *C. albicans* biofilms and have been shown to exhibit increased levels of expression during the hyphal transition (50, 51, 65). Therefore, anti-biofilm compounds might be expected to suppress this induction rather than enhance it. However, five of the target genes tested exhibited an increase in expression relative to control cells under inducing conditions. This may be a reflection of the previous observation that HHQ interferes with the later stages of biofilm development (10). Alternatively, this hyper-expression phenotype may affect the capacity of the cell to engineer a community based biofilm. Future studies will focus on elucidating the pathways through which *C. albicans* perceives and responds to challenge with HHQ with the aim of identifying potential therapeutic targets.

Further work using defined *in vivo* models of biofilm and infection will be required to progress the development and evaluation of these small molecules as anti-biofilm compounds. Models are now available for the investigation of infections involving medical devices such as vascular catheters, dentures, urinary catheters, and subcutaneous implants, as well as mucosal biofilm

infections (66). The ongoing development of cell-based or animal models to study *in vivo* infections (66-69), whether as single pathogen or co-culture systems (70), has provided a well-equipped tool-kit for the pre-clinical assessment of these AHQ-based compounds.

Conclusions

In this study, we have functionalized the important microbial signaling molecules HHQ and PQS in order to exploit their interkingdom role to control biofilm formation in *C. albicans*. In addition to deciphering further insights into the molecular mechanism through which these chemical messages elicit a biofilm suppressive response from *C. albicans*, the bioactivity of several lead compounds has provided a viable platform for the development of next generation therapeutics. Crucially, some of these compounds are non-toxic to mammalian cells and have been rendered incapable of activating *P. aeruginosa* virulence systems, thus highlighting their potential utility as an effective therapy combatting human infection.

Author Contributions

FJR, GPM and FOG conceived and designed the investigation. FJR, JPP, LG, and DW performed the biological experimentation, while RC, RS, and EOM conducted the chemical synthesis. FJR, JPP and FOG wrote the manuscript and all authors read and edited the final draft.

449 **References**

450 1. **Cooper MA, Shlaes D.** 2011. Fix the antibiotics pipeline. Nature **472:**32.

451 2. **ECDC/EMEA.** 2009. The bacterial challenge: time to react. European Centre for
452 Disease Prevention and Control and Europrean Medicines Agency, Stockholm.

453 3. **Spellberg B, Powers JH, Brass EP, Miller LG, Edwards JE, Jr.** 2004. Trends in
454 antimicrobial drug development: implications for the future. Clin Infect Dis **38:**1279-
455 1286.

456 4. **Bjarnsholt T, Ciofu O, Molin S, Givskov M, Hoiby N.** 2013. Applying insights from
457 biofilm biology to drug development - can a new approach be developed? Nat Rev Drug
458 Discov **12:**791-808.

459 5. **Davies D.** 2003. Understanding biofilm resistance to antibacterial agents. Nat Rev Drug
460 Discov **2:**114-122.

461 6. **Dong YH, Wang LH, Xu JL, Zhang HB, Zhang XF, Zhang LH.** 2001. Quenching
462 quorum-sensing-dependent bacterial infection by an N-acyl homoserine lactonase. Nature
463 **411:**813-817.

464 7. **Fux CA, Costerton JW, Stewart PS, Stoodley P.** 2005. Survival strategies of infectious
465 biofilms. Trends Microbiol **13:**34-40.

466 8. **Hoiby N, Ciofu O, Johansen HK, Song ZJ, Moser C, Jensen PO, Molin S, Givskov**
467 **M, Tolker-Nielsen T, Bjarnsholt T.** 2011. The clinical impact of bacterial biofilms. Int J
468 Oral Sci **3:**55-65.

469 9. **Rasmussen TB, Givskov M.** 2006. Quorum sensing inhibitors: a bargain of effects.
470 Microbiology **152:**895-904.

10. **Reen FJ, Mooij MJ, Holcombe LJ, McSweeney CM, McGlacken GP, Morrissey JP, O'Gara F.** 2011. The Pseudomonas quinolone signal (PQS), and its precursor HHQ, modulate interspecies and interkingdom behaviour. FEMS Microbiol Ecol **77:**413-428.

11. **Rutherford ST, Bassler BL.** 2012. Bacterial quorum sensing: its role in virulence and possibilities for its control. Cold Spring Harb Perspect Med **2**.

12. **Ternent L, Dyson RJ, Krachler AM, Jabbari S.** 2015. Bacterial fitness shapes the population dynamics of antibiotic-resistant and -susceptible bacteria in a model of combined antibiotic and anti-virulence treatment. J Theor Biol **372:**1-11.

13. **Cox CE, McClelland M, Teplitski M.** 2013. Consequences of disrupting Salmonella AI-2 signaling on interactions within soft rots. Phytopathology **103:**352-361.

14. **Dong YH, Gusti AR, Zhang Q, Xu JL, Zhang LH.** 2002. Identification of quorum-quenching N-acyl homoserine lactonases from Bacillus species. Appl Environ Microbiol **68:**1754-1759.

15. **Hentzer M, Riedel K, Rasmussen TB, Heydorn A, Andersen JB, Parsek MR, Rice SA, Eberl L, Molin S, Hoiby N, Kjelleberg S, Givskov M.** 2002. Inhibition of quorum sensing in *Pseudomonas aeruginosa* biofilm bacteria by a halogenated furanone compound. Microbiology **148:**87-102.

16. **Holcombe LJ, McAlester G, Munro CA, Enjalbert B, Brown AJ, Gow NA, Ding C, Butler G, O'Gara F, Morrissey JP.** 2010. *Pseudomonas aeruginosa* secreted factors impair biofilm development in *Candida albicans*. Microbiology **156:**1476-1486.

17. **Janssens JC, Steenackers H, Robijns S, Gellens E, Levin J, Zhao H, Hermans K, De Coster D, Verhoeven TL, Marchal K, Vanderleyden J, De Vos DE, De**

Keersmaecker SC. 2008. Brominated furanones inhibit biofilm formation by *Salmonella enterica* serovar Typhimurium. Appl Environ Microbiol **74:**6639-6648.

18. **O'Loughlin CT, Miller LC, Siryaporn A, Drescher K, Semmelhack MF, Bassler BL.** 2013. A quorum-sensing inhibitor blocks *Pseudomonas aeruginosa* virulence and biofilm formation. Proc Natl Acad Sci U S A **110:**17981-17986.

19. **Zambelloni R, Marquez R, Roe AJ.** 2015. Development of antivirulence compounds: a biochemical review. Chem Biol Drug Des **85:**43-55.

20. **Desai JV, Mitchell AP, Andes DR.** 2014. Fungal biofilms, drug resistance, and recurrent infection. Cold Spring Harb Perspect Med **4**.

21. **Perlroth J, Choi B, Spellberg B.** 2007. Nosocomial fungal infections: epidemiology, diagnosis, and treatment. Med Mycol **45:**321-346.

22. **Ramage G, Rajendran R, Sherry L, Williams C.** 2012. Fungal biofilm resistance. Int J Microbiol **2012:**528521.

23. **Feldman M, Shenderovich J, Al-Quntar AA, Friedman M, Steinberg D.** 2015. Sustained release of a novel anti-quorum-sensing agent against oral fungal biofilms. Antimicrob Agents Chemother **59:**2265-2272.

24. **Moudgal V, Sobel J.** 2010. Antifungals to treat *Candida albicans*. Expert Opin Pharmacother **11:**2037-2048.

25. **Chandra J, Mukherjee P, Ghannoum A.** 2012. Candida biofilms associated with CVC and medical devices. Mycoses **55:**46–57.

26. **Lynch AS, Robertson GT.** 2008. Bacterial and fungal biofilm infections. Annu Rev Med **59:**415-428.

515 27. **Bink A, Pellens K, Cammue BPA, Thevissen K.** 2011. Anti-Biofilm Strategies: How to
516 Eradicate Candida Biofilms. Open Mycol J **5:**29-38.

517 28. **Finkel JS, Xu W, Huang D, Hill EM, Desai JV, Woolford CA, Nett JE, Taff H,**
518 **Norice CT, Andes DR, Lanni F, Mitchell AP.** 2012. Portrait of *Candida albicans*
519 adherence regulators. PLoS Pathog **8:**e1002525.

520 29. **Miceli MH, Bernardo SM, Lee SA.** 2009. *In vitro* analyses of the combination of high-
521 dose doxycycline and antifungal agents against *Candida albicans* biofilms. Int J
522 Antimicrob Agents **34:**326-332.

523 30. **Bose S, Ghosh AK.** 2011. Biofilms: A Challenge To Medical Science. Journal of
524 Clinical and Diagnostic Research **5:**127-130.

525 31. **Peleg AY, Hogan DA, Mylonakis E.** 2010. Medically important bacterial-fungal
526 interactions. Nature Reviews Microbiology **8:**340-349.

527 32. **Wargo MJ, Hogan DA.** 2006. Fungal--bacterial interactions: a mixed bag of mingling
528 microbes. Curr Opin Microbiol **9:**359-364.

529 33. **Cugini C, Morales DK, Hogan DA.** 2010. *Candida albicans*-produced farnesol
530 stimulates Pseudomonas quinolone signal production in LasR-defective *Pseudomonas*
531 *aeruginosa* strains. Microbiology **156:**3096-3107.

532 34. **Hodgkinson JT, Galloway WR, Saraf S, Baxendale IR, Ley SV, Ladlow M, Welch**
533 **M, Spring DR.** 2011. Microwave and flow syntheses of Pseudomonas quinolone signal
534 (PQS) and analogues. Org Biomol Chem **9:**57-61.

35. **Mashburn-Warren L, Howe J, Brandenburg K, Whiteley M.** 2009. Structural requirements of the Pseudomonas quinolone signal for membrane vesicle stimulation. J Bacteriol **191:**3411-3414.

36. **Reen FJ, Clarke SL, Legendre C, McSweeney CM, Eccles KS, Lawrence SE, O'Gara F, McGlacken GP.** 2012. Structure-function analysis of the C-3 position in analogues of microbial behavioural modulators HHQ and PQS. Org Biomol Chem **10:**8903-8910.

37. **Reen FJ, Shanahan R, Cano R, O'Gara F, McGlacken GP.** 2015. A structure activity-relationship study of the bacterial signal molecule HHQ reveals swarming motility inhibition in *Bacillus atrophaeus*. Org Biomol Chem **13:**5537-5541.

38. **Deziel E, Lepine F, Milot S, He J, Mindrinos MN, Tompkins RG, Rahme LG.** 2004. Analysis of *Pseudomonas aeruginosa* 4-hydroxy-2-alkylquinolines (HAQs) reveals a role for 4-hydroxy-2-heptylquinoline in cell-to-cell communication. Proc Natl Acad Sci U S A **101:**1339-1344.

39. **Diggle SP, Matthijs S, Wright VJ, Fletcher MP, Chhabra SR, Lamont IL, Kong X, Hider RC, Cornelis P, Camara M, Williams P.** 2007. The *Pseudomonas aeruginosa* 4-quinolone signal molecules HHQ and PQS play multifunctional roles in quorum sensing and iron entrapment. Chem Biol **14:**87-96.

40. **McGlacken GP, McSweeney CM, O'Brien T, Lawrence SE, Elcoate CJ, Reen FJ, O'Gara F.** 2010. Synthesis of 3-halo-analogues of HHQ, subsequent cross-coupling and first crystal structure of Pseudomonas quinolone signal (PQS). Tetrahedron Letters **51:**5919-5921.

41. **Pesci EC, Milbank JB, Pearson JP, McKnight S, Kende AS, Greenberg EP, Iglewski BH.** 1999. Quinolone signaling in the cell-to-cell communication system of *Pseudomonas aeruginosa*. Proc Natl Acad Sci U S A **96:**11229-11234.

42. **Fletcher MP, Diggle SP, Camara M, Williams P.** 2007. Biosensor-based assays for PQS, HHQ and related 2-alkyl-4-quinolone quorum sensing signal molecules. Nat Protoc **2:**1254-1262.

43. **Ramage G, Vande Walle K, Wickes BL, Lopez-Ribot JL.** 2001. Standardized method for in vitro antifungal susceptibility testing of *Candida albicans* biofilms. Antimicrob Agents Chemother **45:**2475-2479.

44. **Hawser S.** 1996. Comparisons of the susceptibilities of planktonic and adherent *Candida albicans* to antifungal agents: A modified XTT tetrazolium assay using synchronised C-albicans cells. Journal of Medical and Veterinary Mycology **34:**149-152.

45. **Essar DW, Eberly L, Han CY, Crawford IP.** 1990. DNA sequences and characterization of four early genes of the tryptophan pathway in *Pseudomonas aeruginosa*. J Bacteriol **172:**853-866.

46. **Miller JH.** 1972. Experiments in Molecular Genetics. Cold Springs Harbor Laboratory Press, Cold Springs Harbor NY.

47. **Nett JE, Cain MT, Crawford K, Andes DR.** 2011. Optimizing a Candida biofilm microtiter plate model for measurement of antifungal susceptibility by tetrazolium salt assay. J Clin Microbiol **49:**1426-1433.

48. **Baell J, Walters MA.** 2014. Chemistry: Chemical con artists foil drug discovery. Nature **513:**481-483.

49. **Bandara HM, Cheung BP, Watt RM, Jin LJ, Samaranayake LP.** 2013. Secretory products of *Escherichia coli* biofilm modulate Candida biofilm formation and hyphal development. J Investig Clin Dent **4:**186-199.

50. **Finkel JS, Mitchell AP.** 2011. Genetic control of *Candida albicans* biofilm development. Nat Rev Microbiol **9:**109-118.

51. **Martin R, Albrecht-Eckardt D, Brunke S, Hube B, Hunniger K, Kurzai O.** 2013. A core filamentation response network in *Candida albicans* is restricted to eight genes. PLoS One **8:**e58613.

52. **Nailis H, Coenye T, Van Nieuwerburgh F, Deforce D, Nelis HJ.** 2006. Development and evaluation of different normalization strategies for gene expression studies in *Candida albicans* biofilms by real-time PCR. BMC Mol Biol **7:**25.

53. **Klein T, Henn C, de Jong JC, Zimmer C, Kirsch B, Maurer CK, Pistorius D, Muller R, Steinbach A, Hartmann RW.** 2012. Identification of small-molecule antagonists of the *Pseudomonas aeruginosa* transcriptional regulator PqsR: biophysically guided hit discovery and optimization. ACS Chem Biol **7:**1496-1501.

54. **Lu C, Kirsch B, Zimmer C, de Jong JC, Henn C, Maurer CK, Musken M, Haussler S, Steinbach A, Hartmann RW.** 2012. Discovery of antagonists of PqsR, a key player in 2-alkyl-4-quinolone-dependent quorum sensing in *Pseudomonas aeruginosa*. Chem Biol **19:**381-390.

55. **Lu C, Maurer CK, Kirsch B, Steinbach A, Hartmann RW.** 2014. Overcoming the unexpected functional inversion of a PqsR antagonist in *Pseudomonas aeruginosa*: an in

vivo potent antivirulence agent targeting pqs quorum sensing. Angew Chem Int Ed Engl **53:**1109-1112.

56. **Ilangovan A, Fletcher M, Rampioni G, Pustelny C, Rumbaugh K, Heeb S, Camara M, Truman A, Chhabra SR, Emsley J, Williams P.** 2013. Structural basis for native agonist and synthetic inhibitor recognition by the *Pseudomonas aeruginosa* quorum sensing regulator PqsR (MvfR). PLoS Pathog **9:**e1003508.

57. **McGrath S, Wade DS, Pesci EC.** 2004. Dueling quorum sensing systems in *Pseudomonas aeruginosa* control the production of the Pseudomonas quinolone signal (PQS). FEMS Microbiol Lett **230:**27-34.

58. **Casadevall A.** 1996. Crisis in infectious diseases: time for a new paradigm? Clin Infect Dis **23:**790-794.

59. **Casadevall A.** 2009. The case for pathogen-specific therapy. Expert Opin Pharmacother **10:**1699-1703.

60. **Spellberg B, Rex JH.** 2013. The value of single-pathogen antibacterial agents. Nat Rev Drug Discov **12:**963.

61. **EMA.** 2012. Addendum to the note for guidance on evaluation of medicinal products indicated for treatment of bacterial infections (CPMP/EWP/558/95 REV 2) to address indication-specific clinical data.,

62. **Alemayehu D, Quinn J, Cook J, Kunkel M, Knirsch CA.** 2012. A paradigm shift in drug development for treatment of rare multidrug-resistant gram-negative pathogens. Clin Infect Dis **55:**562-567.

63. **IFDSA.** 2012. White paper: recommendations on the conduct of superiority and organism-specific clinical trials of antibacterial agents for the treatment of infections caused by drug-resistant bacterial pathogens. Clin Infect Dis **55:**1031-1046.

64. **Nett JE.** 2014. Future directions for anti-biofilm therapeutics targeting Candida. Expert Rev Anti Infect Ther **12:**375-382.

65. **Desai JV, Mitchell AP.** 2015. *Candida albicans* Biofilm Development and Its Genetic Control. Microbiol Spectr **3**.

66. **Nett JE, Andes DR.** 2015. Fungal Biofilms: In Vivo Models for Discovery of Anti-Biofilm Drugs. Microbiol Spectr **3**.

67. **Chauhan A, Bernardin A, Mussard W, Kriegel I, Esteve M, Ghigo JM, Beloin C, Semetey V.** 2014. Preventing Biofilm Formation and Associated Occlusion by Biomimetic Glycocalyxlike Polymer in Central Venous Catheters. Journal of Infectious Diseases **210:**1347-1356.

68. **Chauhan A, Ghigo JM, Beloin C.** 2016. Study of in vivo catheter biofilm infections using pediatric central venous catheter implanted in rat. Nature Protocols **11:**525-541.

69. **Kucharikova S, Neirinck B, Sharma N, Vleugels J, Lagrou K, Van Dijck P.** 2015. *In vivo Candida glabrata* biofilm development on foreign bodies in a rat subcutaneous model. J Antimicrob Chemother **70:**846-856.

70. **Sobue T, Diaz P, Xu H, Bertolini M, Dongari-Bagtzoglou A.** 2016. Experimental Models of *C. albicans-Streptococcal* Co-infection. Methods Mol Biol **1356:**137-152.

643 **Table 1. Compound Data**

Compound	Structure	Yield [%][a]	MW	Rf[b]	Class[c]
1	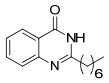	76	244.3	0.319	I
2*	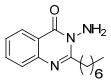	3	259.3	0.907	I
3	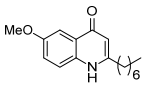	34	273.4	0.252	II
4	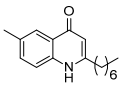	31	257.4	0.286	II
5	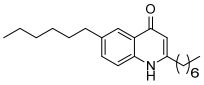	35	327.5	0.504	II
6	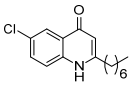	21	277.8	0.403	II
7	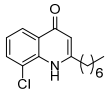	19	277.8	0.630	II
8	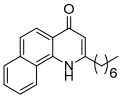	46	293.4	0.294	II

9*	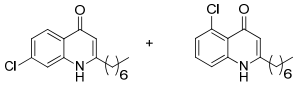	6	277.8	0.361	II
10	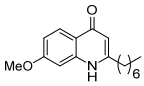	33	273.4	0.261	II
11	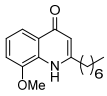	12	273.4	0.504	II
12	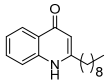	23	271.4	0.395	III
13*	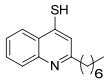	48	259.4	1	IV
14	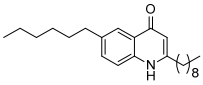	16	355.6	0.538	V
15	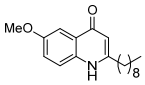	28	301.4	0.286	V
16	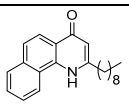	51	321.5	0.462	V
17	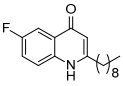	16	289.4	0.504	V

644

645 [a] % yields are isolated yields over all steps

646 [b] TLC on silica plates with Dichloromethane:MeOH (95:5) mobile phase

647 [c] Class I – modified C-3; Class II – modified anthranilate ring; Class III – modified alkyl chain;

648 Class IV – modified C-4; Class V – modified anthranilate ring and alkyl chain.

649 * New compounds synthesized in this study

650

651

652

653

654

655

656

657

658

659

660

661

662 **Table 2. Selective Toxicity Index of Lead Compounds**

Compound	**Selective Toxicity Index**			
	IB3-1	A549	DU145	HeLa
HHQ	**	***	**	****
PQS	*	**	*	*
1	*	*	*	*
2	**	****	****	****
4	*	****	**	****
6	**	***	*	****
9	*	**	*	**
12	**	***	**	****

663

664 % Toxicity * (0-25), ** (26-50), *** (51-75), **** (76-100)

665

666

667

668 **Figure Legends**

669 **Figure 1. *C. albicans* biofilms are altered in the presence of HHQ**. Filamentous *C. albicans*
670 biofilms grown in the presence of PQS and HHQ (100 µM) were assessed structurally by
671 confocal microscopy and metabolically using the XTT biofilm assay. Data (means ± SEM) are
672 representative of three independent biological experiments and are presented relative to the
673 untreated control. Two-tailed paired student's t-test was performed by comparison of *C. albicans*
674 in the presence of HHQ and PQS with *C. albicans* treated with methanol or ethanol (*, p-value ≤
675 0.05).

676

677 **Figure 2. Decoration of HHQ exhibits variable biofilm activity against *C. albicans.* (a)** A
678 panel of HHQ derivatized analogues incubated with filamentous *C. albicans* and screened for
679 biofilm formation using the metabolic XTT biofilm assay. Data is presented as OD_{492nm}
680 spectrophotometric output normalized to the untreated control, and is representative of at least
681 three independent biological replicates, with error bars representing SEM. (**b**) Dose-dependent
682 XTT analysis of selected anti-biofilm compounds applied at 10, 50, and 100 µM. Data is the
683 average of at least two independent biological replicates, each constituting eight technical
684 replicates. Statistical analysis of both datasets was performed by one-way ANOVA with
685 Bonferroni corrective testing, and is presented relative to the MeOH control; * $p \leq 0.05$, ** $p \leq$
686 0.01 and *** $p \leq 0.001$.

687

688 **Figure 3. Microscopic analysis reveals altered biofilm structures.** Analogues that lead to
689 reduced *C. albicans* biofilm formation in the XTT assay (**1**, **2**, **3**, **4**, **6**, **7**, **9**, **12**, and **15**) exhibit
690 compromised biofilm structures. Filamentous *C. albicans* biofilm in the presence of analogues
691 (100 μM) was stained for chitin and cellulose (calcofluor; blue), lectins which binds to sugars,
692 glycolipids and glycoproteins (concanavalin A; green) and live-dead cells (FUN-1; red).

693

694 **Figure 4. Hyphal pathway genes are hyper-expressed in response to HHQ.** Transcript
695 expression analysis (Real Time RT-PCR) of a panel of biofilm genes was assessed in *C. albicans*
696 grown in YNB-NP (filamentous inducing media) in 100 μM HHQ for 6 hours at 37°C. All data
697 was normalized to a housekeeper gene (*ACT1*). Error bars represent SD of three independent
698 biological replicates. Two-tailed paired student's t-test was performed by comparison of HHQ
699 treated cells with methanol control in YNB-NP inducing medium (*, p-value ≤ 0.05).

700

701 **Figure 5. Cytotoxicity towards specific mammalian cell lines is reduced in lead compounds.**
702 **(a)** Cytotoxicity, measured as a percentage of total lactate dehydrogenase (LDH) released from
703 IB3-1 cells treated with 0.1% Triton X-100 (100% cytotoxicity), was significantly reduced in the
704 presence of several lead compounds. Data (means ± SEM) are representative of three
705 independent biological experiments. **(b)** Selected lead compounds were tested against A549,
706 DU145, and HeLa cell lines. Data represents four independent biological replicates and all
707 datapoints are normalized to Triton X-100 as above. A one-way ANOVA was performed with

708 Bonferroni corrective testing on all datasets and comparison relative to MeOH control is
709 presented; * $p \leq 0.05$, and *** $p \leq 0.001$.

710

711 **Figure 6. Influence of HHQ analogues on PQS-dependent virulence phenotypes in *P.***
712 ***aeruginosa*.** (**a**) Phenazine production and (**b**) *pqsA-lacZ* promoter activity quantified in a PAO1
713 *pqsA* mutant in the presence of HHQ, PQS and lead compounds. Data is presented as mean +/-
714 SEM and is representative of at least three independent biological replicates. A one-way
715 ANOVA was performed with Bonferroni corrective testing and statistical significance relative to
716 the MeOH control is presented; ** $p \leq 0.01$ and *** $p \leq 0.001$.

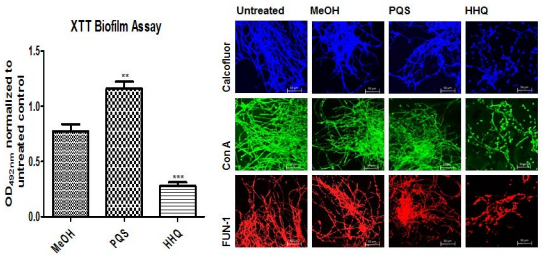

Figure 1. *C. albicans* biofilms are altered in the presence of HHQ. Filamentous *C. albicans* biofilms grown in the presence of PQS and HHQ (100 μM) were assessed structurally by confocal microscopy and metabolically using the XTT biofilm assay. Data (means ± SEM) are representative of three independent biological experiments and are presented relative to the untreated control. Two-tailed paired student's t-test was performed by comparison of *C. albicans* in the presence of HHQ and PQS with *C. albicans* treated with methanol or ethanol (*, p-value = 0.05).

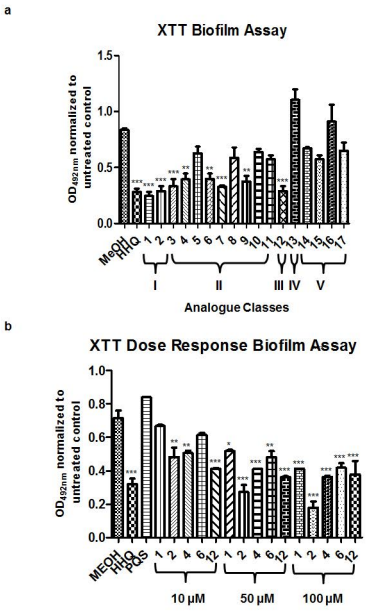

Figure 2. Decoration of HHQ exhibits variable biofilm activity against *C. albicans*. (a) A panel of HHQ derivatized analogues incubated with filamentous *C. albicans* and screened for biofilm formation using the metabolic XTT biofilm assay. Data is presented as OD_{492nm} spectrophotometric output normalized to the untreated control, and is representative of at least three independent biological replicates, with error bars representing SEM. (**b**) Dose-dependent XTT analysis of selected anti-biofilm compounds applied at 10, 50, and 100 µM. Data is the average of at least two independent biological replicates, each constituting eight technical replicates. Statistical analysis of both datasets was performed by one-way ANOVA with Bonferroni corrective testing, and is presented relative to the MeOH control; * $p = 0.05$, ** $p = 0.01$ and *** $p = 0.001$.

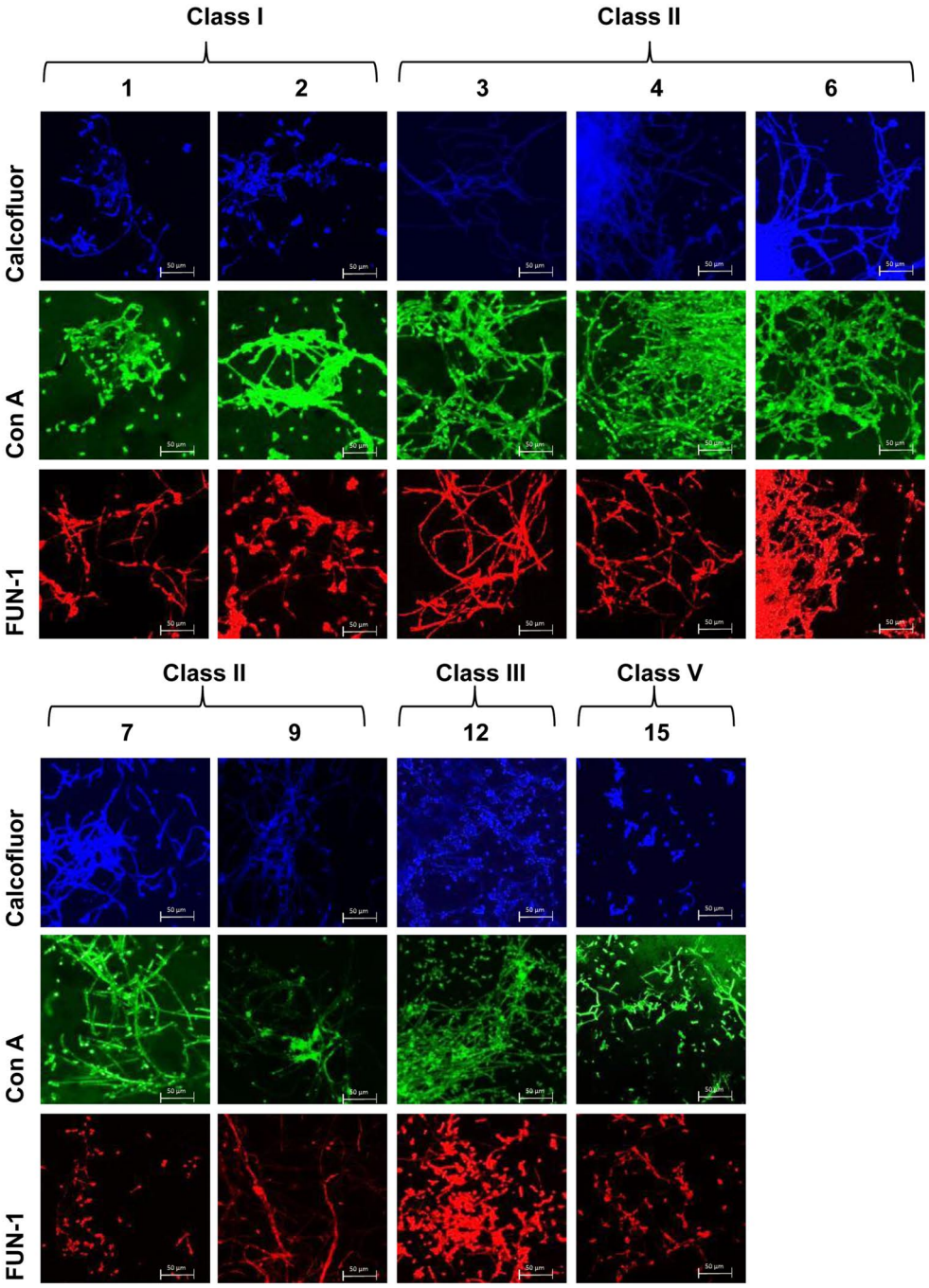

Figure 3. Microscopic analysis reveals altered biofilm structures. Analogues that lead to reduced *C. albicans* biofilm formation in XTT assay (**1**, **2**, **3**, **4**, **6**, **7**, **9**, **12**, and **15**) exhibit compromised biofilm structures. Filamentous *C. albicans* biofilm in the presence of analogues (100 μM) was stained for chitin and cellulose (calcofluor; blue), lectins which binds to sugars, glycolipids and glycoproteins (concavalinA; green) and live-dead cells (FUN-1; red).

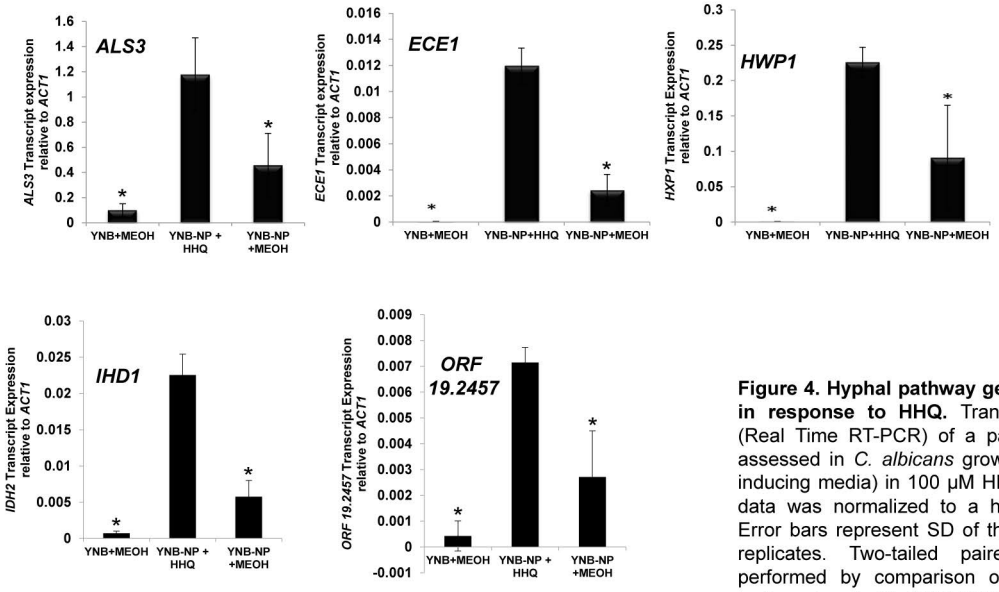

Figure 4. Hyphal pathway genes are hyper-expressed in response to HHQ. Transcript expression analysis (Real Time RT-PCR) of a panel of biofilm genes was assessed in *C. albicans* grown in YNB-NP (filamentous inducing media) in 100 μM HHQ for 6 hours at 37°C. All data was normalized to a housekeeper gene (ACT1). Error bars represent SD of three independent biological replicates. Two-tailed paired student's t-test was performed by comparison of HHQ treated cells with methanol control in YNB-NP inducing medium (*, p-value ≤ 0.05).

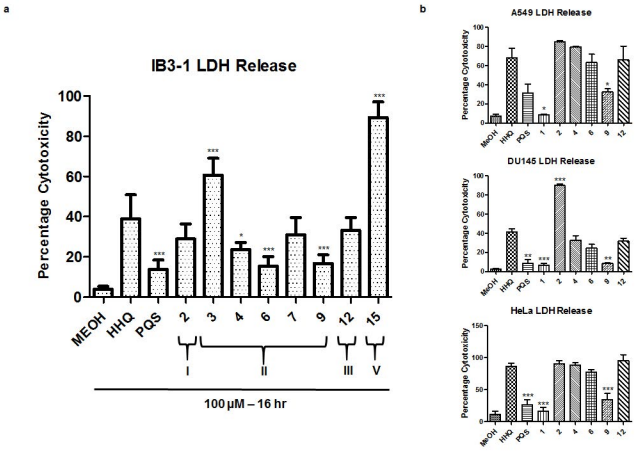

Figure 5. Cytotoxicity towards specific mammalian cell lines is reduced in lead compounds. **(a)** Cytotoxicity, measured as a percentage of total lactate dehydrogenase (LDH) released from IB3-1 cells treated with 0.1% Triton X-100 (100% cytotoxicity), was significantly reduced in the presence of several lead compounds. Data (means ± SEM) are representative of three independent biological experiments. **(b)** Selected lead compounds were tested against A549, DU145, and HeLa cell lines. Data represents four independent biological replicates and all datapoints are normalized to Triton X-100 as above. A one-way ANOVA was performed with Bonferroni corrective testing on all datasets and comparison relative to MeOH control is presented; * $p = 0.05$, and *** $p = 0.001$.

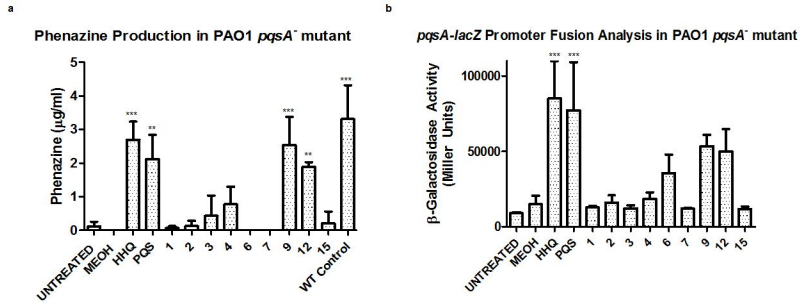

Figure 6. Influence of HHQ analogues on PQS-dependent virulence phenotypes in *P. aeruginosa*. (**a**) Phenazine production and (**b**) *pqsA-lacZ* promoter activity quantified in a PAO1 *pqsA* mutant in the presence of HHQ, PQS and lead compounds. Data is presented as mean +/- SEM and is representative of at least three independent biological replicates. A one-way ANOVA was performed with Bonferroni corrective testing and statistical significance relative to the MeOH control is presented; ** $p = 0.01$ and *** $p = 0.001$.